What can we learn from combined SAXS and SANS measurements of the same sample containing surfactants?

To cite this article: Thomas Zemb and Olivier Diat 2010 *J. Phys.: Conf. Ser.* **247** 012002

View the article online for updates and enhancements.

What can we learn from combined SAXS and SANS measurements of the same sample containing surfactants?

Thomas Zemb and Olivier Diat

Institut de Chimie séparative de Marcoule, UMR5257 CEA/CNRS/UM2/ENSCM, F30207 Bagnols sur Cèze (France)

thomas.zemb@icsm.fr

Abstract. We review the information gained when studying the same sample containing surfactants by SANS and SAXS. Specific information can be obtained if intensities I(q) are determined and used on absolute scale as well as over a large q-window, thus extending to the « Porod limit » asymptotic range. Comparing SAXS and SANS peak positions (when present) allows unambiguous identification of structure factors separated from underlying form factors. Absolute scale refers to scattering cross-section while resolution relates to the q_{max}/q_{min} ratio. Taking into account "external" knowledge of molecular volumes in constrained fitting from explicit models gives better results on aggregation numbers as well as on interfacial thickness than considering only Patterson functions.

We assemble in this review results on adsorption isotherms on surfactant films as well as equations of state, quantifying colloidal interactions. Identification of the topological origin of swelling behaviour are made possible by using combined SAXS and SANS on the largest possible q-range. Best results using this general methodology up to now were obtained by considering data separated from background up to q_{max}= 0.6 Å^{-1} - 0.8 Å^{-1}.

1. Structure factors and dilution plots

In the seventies, "vesicles" and "micelles" made from amphiphilic molecules were not distinguished because of the similarities and interplay between core-shell form factors dominating the SAXS signal and the structure factor more apparent in SANS. Broad peaks observed typically in the range q= 0.01 Å^{-1} to q= 0.1 Å^{-1} arise either from the structure factor S(q) or from the from factor P(q) due to the high electron density present in polar head-groups. Comparing SAXS and SANS spectra from the same sample allowed for the first time direct separation between form and structure factors. As a direct extrapolation of this separation procedure, it has been demonstrated that decomposition in form and structure factors – initially introduced for discrete globular particles by Hayter and Penfold [1], remains valid for connected structures. In this case, space has to be tessellated in Voronoï cells of density n. Average distance between cell centres is, in that case, the origin of the maximum of structure factors [2]. The structure factor S(q) gives information on the network of cell centres, which is Fourier transformed to obtain the pair correlation function $\gamma(\vec{r})$. On this lattice, any set of connected structures is geometrically convoluted by a local microstructure: this can be either a droplet, a connected cylinder or a connected bilayer at first approximation. The product of the underlying S(q), the distribution of seed points, by the local shape characterized by P(q) corresponds still to the experimental I(q) at a very good approximation. This has been numerically verified by Welberry [2] and Barnes [3]. This applies to most micelles and

microemulsions in the bicontinuous [4], including those with a stiff interfaces, where bending energy overcomes entropy effects. [1, 5].

The implicit decomposition of a random network into local structure convoluted on a set of seed points is schematised on figure 1: on the left part, a typical tesselation of space in adjacent cells is shown. Each of these Voronoi cells may be decorated with a droplet at centre, or connected cylinders perpendicular to cells faces or swollen bilayers decorating the faces. The 2D (or 3D) structure can further be described by a connectivity Z or a symmetry ψ, characterizing the dissymetry of the two spaces on both sides of the interface. Figure 1 to the left shows local microstructures as connected cylinders with Z=2, alias a living polymer or fluid giant micelle (top) or a connected cylinder microstructure with connectivity 4 (bottom), which can be understood as a molten cubic phase with local diamond structure. If the maximum in SAXS and SANS coincides, this can be identified safely as a measure of the most probable distance between centres of Voronoï cells.

From the plot of the scaled peak position D*. Σ versus volume fraction ϕ, such as the one shown on figure 1 (central part), different types of microemulsions can be discriminated, since the swelling depends on the dimensionality of the aggregates. Reduced units must be used in so-called "swelling plots", which links the dimensionless product of the peak position by the specific water/oil interface versus the specific volume Σ, in units of area per unit volume (reciprocal length). Power-law description of swelling law versus volume fraction is simple in the case of droplets (slope: -1/3), cylinders (-1/2) or smectics (-1). However, all intermediary values exist: swelling plots can be used to identify local dimensionality of the microstructure [2].
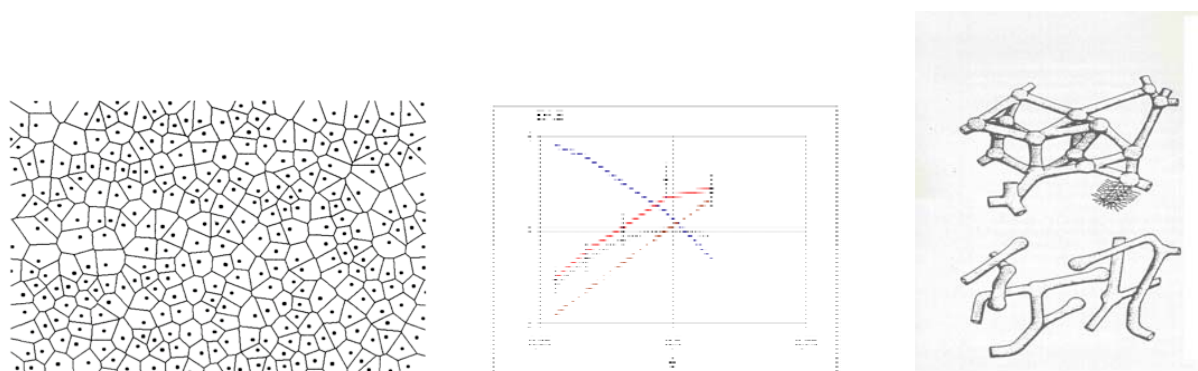

Figure 1. Left: 2D-model of a Voronoï tesselation of space: partition of each Voronoï cell in a « polar » and « non-polar » part separated by a film allows to build a complete family of connected structures of known volume fraction ϕ, specific surface and structure factor. Middle: Comparison of an experimental swelling curve, linking scattering peak position D*. Σ (-S/V) to volume fraction ϕ, to the expected behaviours expected from different types of microemulsions. Continuous line: DOC locally lamellar model; double-dotted increasing line: water-in oil spheres; triple-dotted decreasing line: biliquid o/w foam, thin dotted line: standard flexible model of microemulsions using De Gennes-Taupin prediction. Right: scaled sketches of randomly connected locally cylindrical w/o microemulsions. Top: a "molten" cubic phase; bottom: a living polymer, with connection points and end-caps [reproduced from 5 and 17].

In the case of small droplet micelles formed by surfactants, it has been shown by Hayter and Penfold [1] that self-consistent fitting on absolute scale has not to rely on adjustment of radii, but only of aggregation and hydration numbers. This allows to define uniquely the intermediary values with a physical meaning such as radii and scattering length densities [6]. There are two ways to generate simulated I(q) for micellar systems: one method is to choose arbitrarily "best" radii for SAXS and SANS, these are different because excess electron relevant in SAXS density profiles are not proportional to scattering length density profiles relevant for SANS. The other method is to use number of molecules –i.e. surfactant, co-surfactant, "bound" water molecules per aggregate (or area per head-group). Using known molecular volumes, one calculates then the radii of the "core" and the "shell" of micelle as a function of aggregation numbers, hydration numbers, and fraction of bound

counter-ions only. Typically radii involved are of the order of nanometre; therefore in the classical q-range up to 0, 6 Å^{-1}, one gains no information on attempting to separate micelle in a third layer, such as Palisade or Stern layer. Such details are beyond resolution of SAXS/SANS if the q-range considered is not extended above 0.6 Å^{-1}. Since chemical formulae of molecules involved are known, and when proton exchange or counter-ion distributions are taken into account, the scattering length densities are calculated by simple addition and are not fitting parameters. Hence, SAXS and SANS can be calculated together –using the same S(q) of course- for one unique choice of aggregation and hydration numbers [7]. Simultaneous fit on absolute scale and over the whole q-range ensures consistency of the result and good determination of micellar structure. Any procedure allowing arbitrary fitting on radii and scattering length density may produce inconsistent values of radii and masses. The result coming out may be perfect reproduction of scattering curves, but with values inconsistent with known molecular volumes taken from density or area par head-group, specially if SANS or SAXS data are fitted "alone".

On figure 2, we show an example for a typical surfactant micellar system (20g/l), the broad scattering peak observed by SAXS and SANS are of different origin. However, the same S(q) comes in the form factor-structure factor iterative separation procedure and the two spectra are well fitted by the same ensemble of hydration numbers, aggregation numbers and effective charge parameters [7,8, 9]. In the same approach, effective charge has to be uniquely defined as the un-compensated charge due to all counter-ions not included in the polar part of the micelle. Thus, fitting simultaneously SAXS and SANS on absolute scale with the same basic quantities, i.e. numbers of molecules and effective charge allows unique determination of osmotic compressibility, charge and mass of micelles.
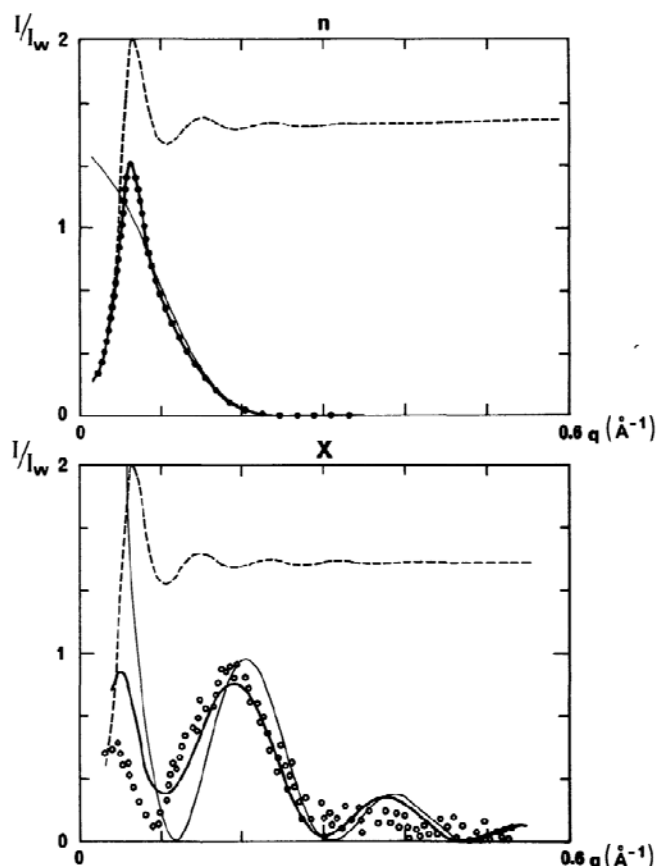
Figure 2. Using the scattering of pure water as a reference as well for SAXS than for SANS, this figure shows that broad peaks observed for some micelles made from single-chain ionic surfactants arise from the structure factor (SANS, upper graph) or from the form factor of a "hollow shell" of head-groups (SAXS, lower graph). Figure shows decomposition in structure (dashed line) and form factors (dotted line), obtained from the same values of fitting parameters: Aggregation number, hydration number and effective charge [extracted from ref. 7].

2. High-resolution combined SAXS and SANS extended to high-q region

On a wide q-range, i.e. for a q_{max}/q_{min} of at least two decades, micellar aggregates can be studied at so-called "high resolution". Figure 3 shows in the right plot, a "Porod plot", the product $q^4 I(q)$ versus q, for diluted ionic micelles versus q. Measurement has to be extended at least up to q= 0.6 Å^{-1} , i.e. the spatial resolution to $2\pi/q_{max}$ of 10 Å. Patterns arising from intra-micellar form factor P(q) clearly differ, as shown on figure 3 (left). Combined with high-resolution SAXS experiments made on the same q-range, data as those shown on figure 3 (left) can be compared to predictions arising from different models of packing of chains in the micellar core.
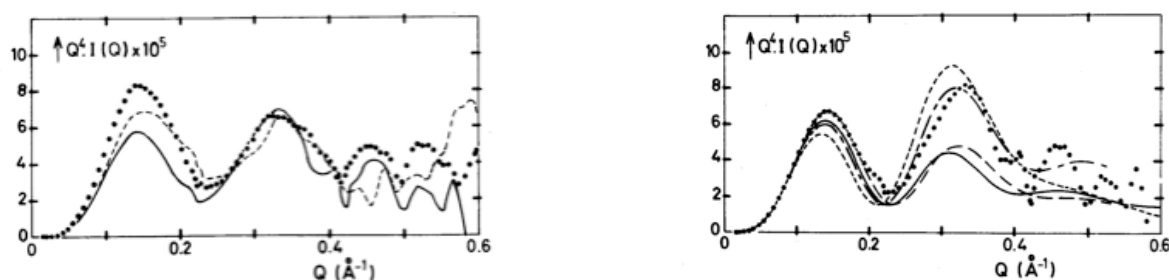

Figure 3. Left: Wide angle neutron scattering (WANS) observed up to large q-window for SDS micelles with specifically labelled groups. The "Porod plot" q4.I(q) versus q enhancing the high-resolution part of the spectrum demonstrates differences in the localisation of the deuterated groups. Right: Comparison between statistical models of packing of chains in the core of micelles illustrates the high degree of disorder in the chains. Dots: full contrast, dashed line: deuterated in position 3; continuous line: deuterated at the end of chain [from ref. 8].

This type of experiments demonstrated that chains in the micellar core are disordered and liquid-like. With a probability of a "gauche" conformation 1/3 along SDS chains, the methylated end-groups are frequently present at the oil-water interface: this explains the "anomalous reactivity" of functional groups attached close to the end-groups of hydrophobic chains in micelles. Thus, for ionic micelles, frequent location of methyl-terminal chains could be ascertained by comparing SAXS and SANS data from specifically deuterated surfactants in D$_2$O solutions up to 0.6 Å^{-1} [8].

In this early work, the thickness of the polar layer made by the head-groups has been determined to be 4 Å in the case of sodium as a counter-ion. In the case of caesium, this may be different. Fitting on absolute scale on the largest available q-range with the SAME input parameters the scattering of a micelle has been performed again by Vass and co-workers using anionic micelles with caesium as a counter-ion: these authors have shown that provided the q-range is extended up to 0.6 Å^{-1}, the layer of caesium as counter-ion can be modelled as a diffuse layer within approximation in standard Poisson-Boltzmann distributions [9]. However, four radial layers where needed to model perfectly the results: the classical core, shell and cation diffuse cloud, but also a fourth layer probably consistent with the Hofmeister effect related to the polarisable caesium ion [10].

Another way to produce more cohesive and diffuse polar layer of micelles is to make catanionics. Salt-free catanionics are produced by using H$^+$ and OH$^-$ counter-ions only while five component catanionic samples are produced by simple mixing of two ionic surfactants. Using a q-range in SANS and SAXS extending up to q= 0.6 Å^{-1}, it has been possible to determine the "thickness" of the layer made by charged polar heads in the case of catanionic micelles. The "diffusivity" of mixtures of anionic and cationic surfactants, i.e. catanionic bilayers above chain melting temperature, has been studied by using a similar combined SAXS-SANS methodology, but without the constraint in fitting given by known molecular volumes, and therefore calculating normalized Patterson functions. Kaler and co-workers have found that head-groups form a diffuse boundary when 5% salt is added, i.e. that the layer formed by head-groups has an extension similar to the Debye screening length, a value compatible with expected cohesive energies of surfactants [11]. It is important to notice that close to

equimolarity, the thickness of the "polar" layer sometimes called "Palisade layer" is typically double for catanionics than for anionic or cationic micelles including quaternary ammoniums or sulfate head-groups only, going from 5Å to 9Å. To our knowledge, these polar layer thicknesses have not yet been determined with sufficiently high resolution - i.e. extending the q-range up to 1 Å^{-1} - in the case of surfactants with variable charge depending on pH, such as phosphates or phosphonates, or when variable chain aliphatic alcohols are added.

What happens wit the polar layer thickness and the curvature when the micelle is "stabilized" by polymerisation of its constituent? To answer this question, polymerisable catanionic mixtures were studied comparing absolute scale of the scattering differing in SAXS and SANS. Unfortunately, the q-range of measurement only extended to 0.3 Å^{-1}, so the associated spatial resolution is 20 Å. However, it could be confirmed that whatever composition, structure of micelles and microemulsions where conserved upon partial polymerisation of the surfactants [**12**].

The so-called Brij 700 is an important "giant surfactant", with C18 chains counter-balanced by hundred oxyethylen groups. Each micelle is stabilized with a nonionic brush. SANS-SAXS experiments were performed on absolute scale and successful models could only be applied after taking into consideration the crossed terms in form factor as well as the contribution of corona on the average "background solvent" cross-section term. It was shown that corona properties diverge only close to phase inversion temperature (PIT), i.e. within 5°C, associated to dehydration of ethoxy groups. This observation questions the usual assumption about the linearity of spontaneous dependence of interfacial curvature which is usually assumed for non ionic microemulsions [**13**]. In continuity with the study of protruding EO chains, Arleth and co-workers have studied by SAXS/SANS experiments the interfacial thickness of hairy mixed micelles containing PEGylated lipids, proposed to be used as "stealth" liposomes in emerging drug delivery technology. Using Patterson functions, it was found that spheres or cylinders can be observed by varying the mole ratio between the two components. Whatever the shape of the aggregate, the stabilizing protruding chains where interpenetrating and remain Gaussian chains with constant gyration radius even in concentrated solutions. These micelles are stabilized as osmotic brushes [**14**].

In the microemulsion regime, adding Brij700 is a well known method used in industry to increase the « efficiency » of a surfactant mixture: it is supposed intuitively that protruding ethoxy brushes act as stabilizers for droplets. Due to the difficulty of making osmotic measurement with systems containing C$_{12}$E$_5$ nonionic surfactants, only combined SAXS and SANS can directly proven the mechanism, since in light scattering, interaction and structure are intrinsically mixed in the q-range available. They used a q-range up to 0.3Å-1 for microemulsions of 50 Å minimum curvature radius, i.e. a packing parameter of the order of 0.8. With Brij load up to 5% in mass, a rod to sphere transition as well as an increase of repulsion between corona-stabilized micelles could be demonstrated. Quantitative determination of corona extension as well as height of repulsive potential resulting would require higher q-range measurements [**15**].

Extending this methodology, SAXS and SANS experiments have both be performed up to the high-resolution limit. Both intensity curves can then be divided ($I_{SANS}(q)/I_{SAXS}$ (q)) and the resulting ratio is exempt from S(q). This ratio can be compared to the "predicted" from any assumed microstructural molecular packing model, moreover independent from colloidal scale interactions governing the structure factor. Figure 4 shows the case of introducing a small amount of water (typically 10%) in a pure liquid non-ionic surfactant, which is liquid at room temperature and miscible to water at any proportion in a given temperature range. The data obtained have been compared to all proposed structural and thermodynamic models of water-surfactant miscibility, at least in water-poor or solvent-poor domains of ternary phase diagrams. As can be seen in figure 4, all current models up to now models fail to predict the observed ratio $I_{SANS}(q)/I_{SAXS}$ (q) [16]. We believe that this division method on absolute scale and at high resolution remains one of the most powerful methods to investigate concentrated isotropic solutions, involving short surfactant or hydrotrope species, including water-alcohol mixtures.
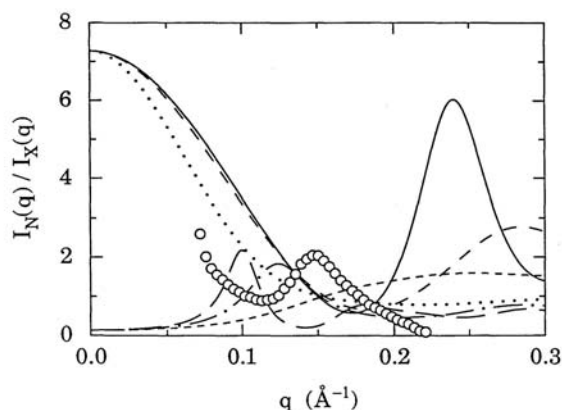
Figure 4. Dividing the SANS by the SAXS spectrum obtained in the same q-range gives a signal depending on P(q) only: this allows a critical test and challenges the models of microstructure in concentrated solutions. The figure shows the failure of currently accepted models of packing to predict the features of IN(q)/Ix(q) in the case of 20% of water added to pure non-ionic surfactant [from ref. 16].

3. Usage of Porod plots to determine thermodynamic quantity: area per surfactant.

Absolute scaled calculations of expected intensities derived from moles to be tested and comparing data on logarithmic scale allows determination of the so-called Porod limit. If investigated aggregate has typical radius R, the asymptotic Porod domain starts for qR above 6 to 10. In some cases, these values obtain by SAXS or SANS differ in quantities as soon as curvatures are large (packing parameters differing from one). From differential geometry, the difference between the values is a direct way to measure curvature and hence determination the packing parameter of the surfactant film. The quantities that have to be known to derive safely specific area per volume of sample (S/V), or per surfactant are either:
  - the electron densities (or scattering length) difference between both sides of the water-oil interface
  - the "invariant" of the full spectrum, i.e. the second moment of the scattering spectrum I(q) which is known from composition [17].

Measuring a sample in the Porod regime requires good statistics for subtracting the background. Often, experiment give more than the expected value. It is always worth to investigate this difference: corrections due to precise determination of solvent scattering length densities for example evidence initially unexpected monomer-aggregate equilibrium. An example along a dilution line in a ternary system involving a cationic synthetic lipid, water and oil is shown on figure 5. As can be seen in log-log plots, the Porod asymptote occurs in over three decades in intensity. The peak positions can be determined by SAXS and SANS, since they occur at similar positions in q-space and may even be refined considering the small correction by taking the maximum of I(q) divided by a good approximation of form factor. This correction rarely exceeds a few percent. It should be mentioned that fitting of data in q-space versus radii only is often made on linear scale, plotting the fit and data on logarithmic scale shows inconsistency: intensity can be easily misevaluated in the high-q part of the region. This is because surfactant assembly has to be characterized with three parameters: one linked to volume, one to curvature and one to available area in the most general case [18].
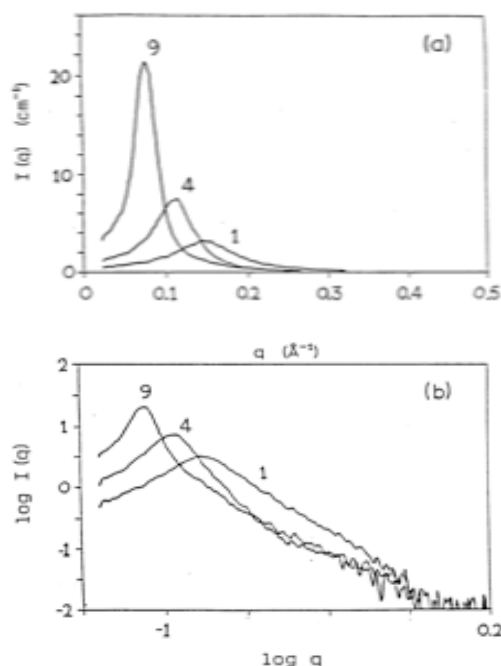
Figure 5. Linear and logarithmic plot of the Intensity I(q) in cm-1, along a dilution line in a ternary or quaternary system allows to determine independently specific surface and "lattice constant" of the underlying Voronoï (or generalized Wigner) cells. Product of peak position by specific surface gives a dimensionless number, crucial for evaluating the swelling behaviour of microstructures [from ref. 18].

The amount of surfactant participating in the surfactant film has in a first step to be separated from the surfactant present as monomers in the "solvent" phase. Once this is taken into account, determination by SAXS and SANS of the basic thermodynamic quantity, i.e. the area of interface per surfactant (or lipid) head participating to the continuous film, can be determined safely with a 10% precision. When compared to values determined on a "flat" -i.e. macroscopic- interface as derived from water-oil surface tension measurements, combined SAXS and SANS experiments performed in the high-q regime allows the determination of the position of the neutral plane of bending. This gives access to the molecular origin of the bending mechanism of surfactant films.

Moreover, the total water-oil contact area per unit sample volume, i.e. the available area (S/V) can be scaled to the peak position, a dimensionless number is then obtained. When microemulsions are made from flexible films, De Gennes and Taupin have demonstrated that this numerical value cannot exceed three [18] (see figure 6).
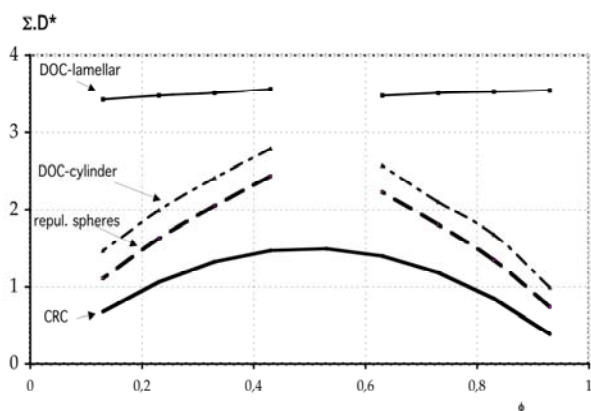

Figure 6. Swelling of the most popular models of microemulsions: the cubic random cell model (CRC, alias De Gennes and Taupin, based on thermodynamics and valid for flexible films; repulsive spherical droplets, connected DOC-cylinders or DOC-lamellar (alias "sponge" phases). The more connected the structure, the higher the value of the dimensionless product .D* [from ref. 17].

More complex structures, which can be understood as molten liquid crystals, "consume" more contact area per unit volume. Hence, the corresponding dilution plot lies above the De Gennes-Taupin relation. De Gennes and Taupin have given a simple analytic expression. Validity is implicitly assumed in most microemulsion studies, such as those implying single-chain non-ionic surfactants [19-20]. However, a large number of results in the literature correspond to other behaviour of swelling plots, meaning that the microemulsion is not made only from a flexible film: curvature effects have to be taken into account. To our knowledge, realistic space representations of random as well as connected structures, thermodynamically equilibrated, and made outside of the degenerated symmetric volume fraction of 50% polar/apolar volume have only be performed once [21].

Establishing experimentally and calculating from random wavelet models dilution plots in scaled units involving only polar/apolar volume fraction and the product of specific area to S(q) peak position translated from reciprocal to real space, has for example allowed to identify the geometrical packing constraints involved in progressive structural transition form globules to connected cylinders and bilayers, a reminiscence of the universal series of liquid crystal structures encountered with co-polymers. Moreover, the procedure introduced by Marcelja allows to represent in real space equilibrium microstructures corresponding to an imposed peak position (using random wavelets) as well as volumes and surfaces for any value of volume fraction, stiffness and spontaneous curvature [21].

For a peculiar class of micelles, known as water-poor w/o microemulsions, used industrially in liquid-liquid extraction processes, simultaneous fitting of I(q) with a large dynamic range in q-space (i.e. $q_{max}/q_{min} > 30$) with the same parameters on an absolute scale allows, on small reverse micelles, unprecedented analytic results. For instance, the effective packing parameter of the highly curved surfactant film can be derived from simultaneous SAXS and SANS modelling, using aggregation numbers as parameters instead of the usual core-shell radii and scattering length densities. The classically considered equation of state relies on osmotic pressure, temperature and the average density between colloidal aggregates. A more delicate thermodynamic relation is the "lateral" equation of state, linking osmotic pressure, temperature and the area per molecule. We have shown that SAXS/SANS comparison allows for the first time, to our knowledge, derivation of not only "perpendicular", but also the "lateral" equations of state governing reverse micelle stability [4].

4. Adsorption isotherms in complex as deduced from combined SAXS and SANS contrast variation

Contrast variation in small angle scattering dates back to sugar/water mixtures used in the investigation of bilayers by Vittorio Luzzatti and co-workers. Serendipously, it was found at that occasion that equilibrium distances between bilayers were strongly increased by the difference in dielectric constants in the van der Waals forces as well as the hydration force between lipid aggregates. Contrast variation, using H/D contrast and specific labelling came into a major technique in physical chemistry and structure determination: from the simple mixture of surfactants [22] to complex structures such as the ribosome [23].

Adsorption of any solute on a pre-existing micelle or microemulsion can be considered with the same concepts than adsorbtion of molecules from a gas or liquid phase on a solid. Combined SANS and SAXS experiments provide an extremely, general and powerful method for direct determination of the adsorption isotherm on any interface made from a surfactant film.

The principle is as follows: Consider for example a lamellar phase in equilibrium with excess water. Then add a solute. The solute may be depleted or adsorbed in the multi-layered vesicle (i.e. the lamellar phase) in equilibrium with excess water. This can be quantified by dosage of the rest of the solute in the excess phase. In parallel, the periodicity shifts to lower values if the solute penetrates in the film and acts as a co-surfactant while periodicity increase if the solute only weakly adsorbs on the surfactant. Accurate SAXS recording of the low-q or high-q peak position shift induced by addition of a solute allows the determination of a possible insertion of the solute in the bilayer (or cylindrical core in the case of an hexagonal phase). For example, partial penetration of hydrophobically modified cyclodextrins were obtained by this method [24]. But how is it possible to determine the adsorption isotherm, i.e. weak adsorption of the solute onto a bilayer?

This has been shown to be possible if one takes into account following observation: if a solute is mixed to the solvent inside a bilayer, it participates to the average scattering length density of the solvent. On the contrary, any solute "bound", i.e. with an interaction energy larger than k_BT towards the interface, the scattering length density of the solute participates to the scattering length density of the periodic bilayer. Using for example H_2O/D_2O mixtures and carbohydrates, or deuterated pentanol, points of zero contrast can vary typically from 5% to 20% in deuterium content [25]. The exact value of zero contrast has to be taken from the square root of intensity at first Bragg peak, and not from the limit at zero-q as usually done in polymer mixtures. Figure 7 shows a contrast plot of this type used to determine adsorption of small sugars onto neutral lipids [26-27]. As an example, depletion from a non-amphiphilic carbohydrate from the interior of a multi-layered liposome could be understood as a simple exclusion from the water in the first shell of hydration of the phospholipids [28]. It should be noted here that "thicknesses" of a heterogeneous bilayer, made from "interior" and "polar head-group" layer, differ naturally if determined by SAXS and SANS: using only the area per head-group and hydration number allows to simulate SAXS and SANS spectra from consistent density profiles. This requires care in using precise definition of the membrane "thickness", since basic variable is area brought per molecule. From this moments of scattering density profiles can be calculated and the same assumption of molecular packing must get to best fitting of scattering data in the high-q regime, as has been shown by Cantu and co-workers [29]. The constraints on acceptable values for the structure of a bilayer, using extra information such as the incompressibility of a fluid with known density are similar in the case of bilayers than the case of micelles as pioneered by Hayter and Luzzatti thirty years ago. This SAXS/SANS method of contrast variation has been extended to investigate hybrid titania/zirconia nanoparticles [30] as well as competitive adsorption of mixed solvents on calcium porous nanoparticles [31].
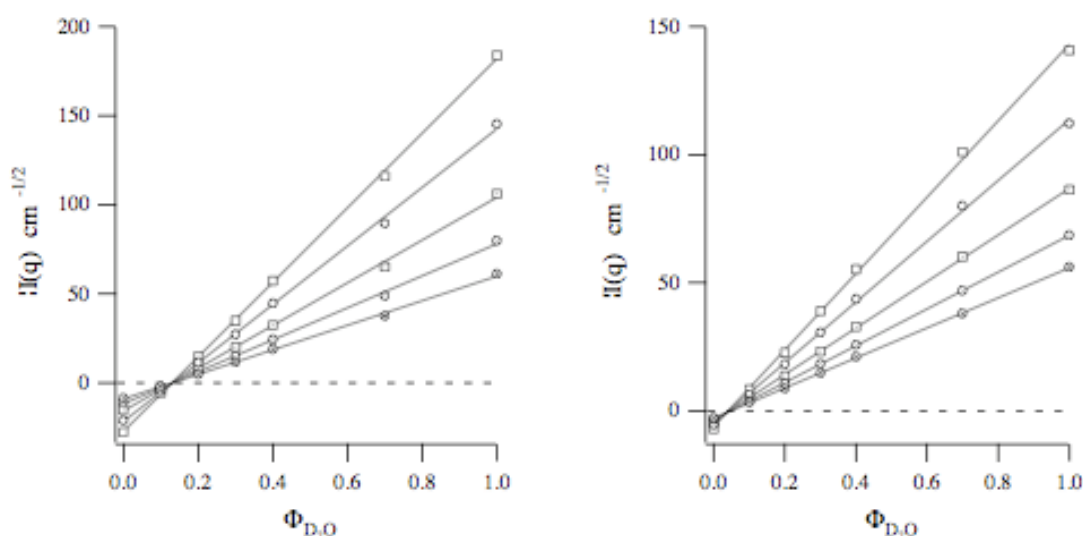

Figure 7. Exact position of match-point during a contrast variation in an organized sample containing a solute depends on the adsorption isotherm of the solute on the water-oil interface. Case of small sugars in phospholipids is shown. The position of the peak as observed by SAXS complements the exact information about periodicity, and detects possible area variations associated to the presence of the solute [from ref. 25].

5. SAXS and SANS experiments to obtain lateral equations of state of surfactants.

The lateral equation of state of surfactant is the relationship between the area per head-group and the osmotic pressure for different temperatures. Only very few complete lateral equations of state are available (see ref. 4 and references cited wherein). An important subset of the lateral equation of state is the relation between molecular area and salinity in the solvent phase. For example in the case of a triple chain lipophilic surfactant, area per molecule and its variation depending on the solute to be extracted in a solvent could be determined using simultaneous SANS and SAXS fitting on an absolute scale. Aggregation numbers, as well as area per head-group tacking into account the volume of the ions and molecules present in the reverse micellar core, could be determined [32-33]. Area per head-group at the water-oil interface, as well as the packing parameter, unambiguously determined from the radii of core and shell of this core-shell structures, have been determined [34]. Figure 8 shows the SAXS and SANS spectra fitted on absolute scale. In this case the scattering from monomers present at high concentration with micelles as well as the crossed term to be considered in the modelisation of scattering to be compared to the experimental results.
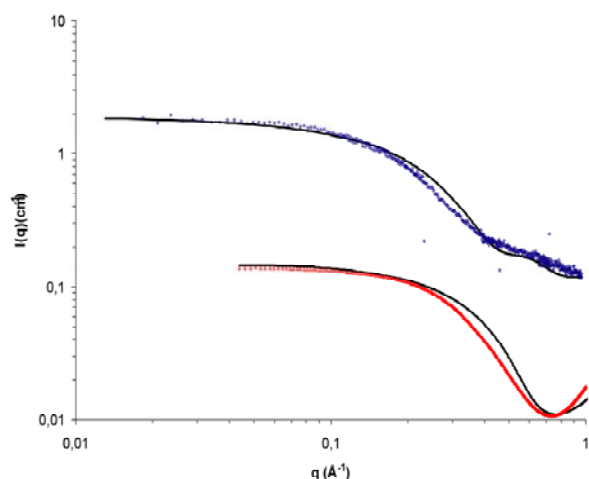

Figure 8. Scattered intensity in log-log and absolute scale in SANS (top) and SAXS (bottom) spectrum of the same reverse micelle, as obtained with a triple chain amphiphilic molecule, compared to models using simultaneous fitting with only one parameter: average aggregation number of the small w/o reverse micelles coexisting with monomers. Solvent is deuterated heptane. Co-solubilized water contained in the core is determined separately by titration [from ref. 34].

The form factor to consider here is the square of the amplitude. The amplitude arising from monomers is not negligible when weak surfactants are considered: typically, one third of the molecules are present in monomers, in coexistence with aggregated pentamers. In this case, form factors of monomers and aggregates, not neglecting the crossed term, has been taken into account in order to obtain agreement of SAXS and SANS on absolute scale. Here again, only aggregation numbers and sticky hard sphere attraction potential compensating sterical repulsions are used as constrained fitting parameters [35]. The sticky hard sphere parameter used in Baxter model can also be determined independently from the phase diagram, knowing the location of the critical point on the liquid-gas transition line of the complex fluid made from reverse micelles [36]. The lateral variation of polar/apolar contact area per molecule and the film curvature (expressed in terms of the dimensionless packing parameter p) are shown in figure 9. Here again, comparison between the "hole in deuterated solvent" as seen by SANS and the volume of the polar core with high electron density as measured by SAXS gives the clue: area per molecule are different at the polar/apolar interface as seen with SAXS, while SANS measures the area of contact of the complete reverse micelle with the solvent [33, 35].
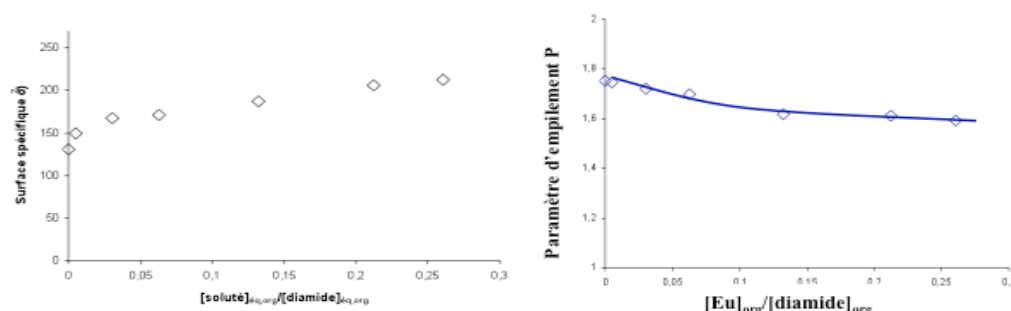
Figure 9. Partial equation of state, related to area and curvature versus ionic strength obtained from simultaneous SANS and SAXS fitting on absolute scale. First direct measure of the effect of ions extracted on the area per head-group versus mole ratio of extracted ions per surfactant as well as interfacial curvature, expressed in terms of dimensionless packing parameter [from ref. 34].

6. SAXS and SANS experiments in frozen surfactant films to determine local order

It has been recently shown that in the so-called "true" catanionic systems, i.e. mixtures of anionic surfactants in acidic form and cationic surfactants presents hydroxide, micelles of different shape are stable as poorly charged colloids, even in the "frozen" state of the surfactant chains. These micelles, prepared by reversible cycling temperatures or soft dialysis are thermodynamically stable. They are in a situation described as gel and sub-gel phases for lipids. Shapes of the micelles depend on the composition and are consistently understood in ternary phase diagrams [37]. Using mixtures of deuterated anionic components and hydrogenated cationic surfactants (or the reverse), fundamental experiments can be done by comparing the Bragg peaks and diffuse scattering. It turns out that SAXS and SANS spectra are complex: interaction peaks, form factors at several scales are seen in SAXS and SANS. Hoverer, extending the q-range of observation to 2.0 Å^{-1} allows observation of Bragg peak by WANS and WAXS: the first order of packing corresponds to hexagonal order of hydrocarbon chains, around 1.6 Å^{-1}. Due to labeling of one of the components, a broad diffuse band appears with a maximum around 0.8 Å^{-1}. This diffuse band is due to local correlation between anionic and cationic components in the plane of head-groups. This diffuse band can be simulated using Monte-Carlo. This broad diffuse band due to the in-plane order of the catanionic bilayer does not exist in the case of random distribution of anions and cations in the plane and sharpens if there is a two-dimensional crystal when mole ratio of component is 2 to 1, analogue to anti-ferromagnetic order. Extreme cases of this shape of the diffuse band seen by WANS are shown in figure 10 [38]. In the present case of local order in frozen chains, it has been shown by combined WANS and WAXS that an in-plane order propagates till the third neighbor.
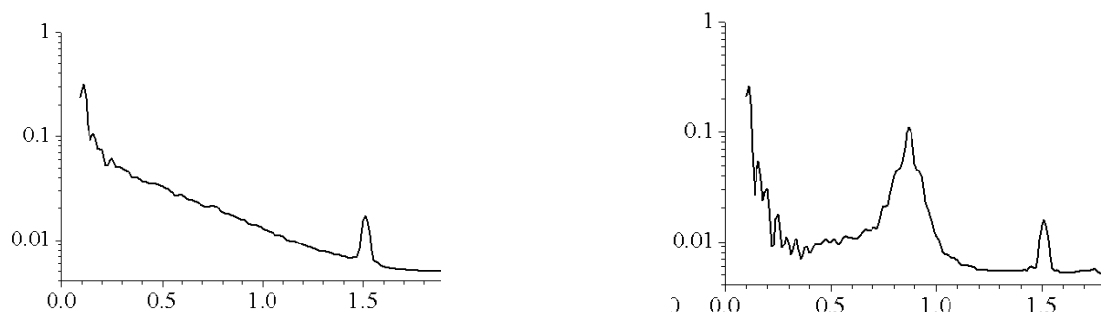

Figure 10. Simulation of diffuse scattering observable in frozen catanionic bilayers at roughly half of the first order in the WANS region due to chain-chain distance. At this q-range, no detection of diffuse scattering is seen in WAXS. Left: limit of random in-plane distribution of anionic and cationic component in a bilayer. Right: with strong correlation due to anionic-cationic component interactions. Comparing simulations to observations of the diffuse band specific of SANS allowed the first determination of the local order in frozen bilayers [from ref. 38].

7. Conclusion

We have shown here that combining SAXS and SANS at high resolution, i.e. up to large q-values and using number of molecules of known chemical composition and molar volume (to be determined by densitometry) gives a very precise description of molecular assembly, including equations of state when osmotic pressure is known.

Using contrast variation, adsorption isotherms on surfactant films as well as location of the solute "in" or "on" the film can be determined. Even with the simplest approach, identification of the maximum of S(q) associated to dilution experiments, can give a direct clue on progressive shape transformations of colloidal aggregates. Combining SAXS and SANS remains one of the most powerful methods for overcoming the mathematical difficulty of getting back to real space from reciprocal space measurements. This is especially relevant if measurements are made on absolute scale, i.e. if scattering cross-sections are experimentally determined using well-defined standards, such as thin layers of pure water at a known temperature, a convenient reference for swollen systems and using SAXS and SANS techniques.

A recent example of this concerns the study maltosides [**39**], single chain amphiphiles. Due to temperature independent hydration of the sugar head-group, packing parameters do not depend on temperature or salinity, making them useful detergents. Using a q-range limited to 0.5Å^{-1}, it has been shown that these molecules form cylindrical micelles with spherical end-caps in water, since the volume of the polar layer is incompressible [40]. What happens when maltosides are mixed with more classical linear nonionic ethoxylates has also been studied by combined SANS-SAXS, taking into account molecular volumes and absolute scale measurements. Surprisingly, instead of the micelle of "average" curvature expected from dynamical equilibrium in micelles, the coexistence of spherical micelles poor in maltoside with cylindrical micelles rich in maltosides, probably enriched at end-caps in one of the components, was recently proposed. This is possible if there are competing attraction/repulsions within the same micelle of the two components; free energy can be minimized by coexistence between A-rich and B-rich micelles of different curvatures in the same sample, still minimizing free energy expressed in the term of packing frustration. Extension to higher q-values and usage of contrast-variation in SANS will probably soon open the door to the first determinations of interaction parameters derived from the structure of micelles: those have to be compared with the one determine from CMC equilibria.

Still a large number of questions in this field are open. For instance, determination of molecular interactions within a given micelle/microemulsions controlling spontaneous packing and coexistence of different micellar shapes –and corresponding solubilisation properties are still ahead!

The review here concerns only surfactants measured by SAXS and SANS: papers are available describing the same SANS/SANS WAXS/WANS methodology used for studying aerogels [**41**], fullerenes [**42**], off-equilibrium coarse emulsions [**43**], rocks [**44**], starch when processed [**45**], and elastomers made from polymers and fillers [**46**]. As can be judged from the variety of colloidal samples investigated, the experimental possibilities opened in the eighties by SANS-contrast variation/SAXS comparison on absolute scale is an emerging methodology which can be used to investigate multi-scale colloidal structures as well as the energetics of the colloidal interaction.

References

[1]   Hayter J B and Penfold R. 1981 *J. Chem. Soc. Faraday Soc.* I **77** 1851
[2]   Welberry T R and Zemb T 1988 *J. Colloid Interface Science* **123** 413 ; Zemb T 1997 *Colloids Surf. A* **129-130**, 435
[3]   Barnes I S and Zemb T 1988 *J. Appl. Crystallogr.* **21** 373
[4]   Chevalier Y and Zemb T 1990 *Reports in Progress of Physics* **53** 279
[5]   Zemb T 1997 *Colloids and Surfaces A* 1997 **129-130** 342
[6]   Hayter J B, Penfold J and Zemb T 1982 *Chem. Phys. Lett.,* **93** 91

[7]   Charpin P, and Zemb T 1985 *J. Physique Paris* **46** 249

[8]   Cabane B, Duplessix R and Zemb T 1985 *J. Physique Paris* **46** 2161

[9]   Vass Sz. *J. Phys. Chem. B* 2001, *105*, 455. ; Vass Sz, Plestil J, Laggner P, Gilanyi T, Borbely S, Kriechbaum M, Jakli G, Decsy Z ,Abuja P M**.** 2003 *J. Phys. Chem. B* **107**, 12752

[10]   Kunz W , in « Specific ion effects », World scientific publ. Singapore (2010)

[11]   Iampietro D J, Brasher L L and Kaler E W, Stradner A and Glatter O, *J. Phys. Chem. B* 1998**,** *102,* 3105

[12]   Summers M, Eastoe J, Davis S, Du Zhipig, Richardson R M, Heean R K and Steytler D, 2001, *Langmuir* **17**, 5388

[13]   Sommer C, Pedersen J S and Garamus V M, 2005 *Langmuir* **21**, 2137

[14]   Arleth L, Ashok B, Onyuksel H, Thiyagarajan P, Jacob J and Hjelm R P, 2005 *Langmuir* **21**, 3279

[15]   Sommer C, Deen G R, Struntz O., Pedersen J S and Garamus V M, 2007 *Langmuir* **23**, 6544

[16]   Barnes I S , Corti M, Degiorgio V and Zemb T 1993 Progr. Colloid Polym. Sci. **93** 205

[17]   Spalla O 1991 in *"Neutron, X-Rays and Light Scattering"*, ed. P. Lindner and T. Zemb, publ. Elsevier 177

[18]   Barnes I S, Derian P J, Hyde S T, Ninham B W and Zemb T 1990 J. Phys. France **51** 2605

[19]   Zemb T 2009 *Comptes Rendus Chimie* **12** 218

[20]   Welberry T R and Zemb T 1993 *Progr. Colloid Polym. Sci.* **271** 124

[21]   Arleth L, Marcelja S and Zemb T 2001 *J. Phys. Chem.* **8** 3923

[22]   Hayter J B, Chevalier Y and Zemb T 1984 *Colloid & Polymer Sci* **262** 798

[23]   May R 1991 in *"Neutron, X-Rays and Light Scattering"*, ed. P. Lindner and T. Zemb, publ. Elsevier 214

[24]   Auzely-Velty R, Djedaini-Pilard F, Taché O, Zemb T, Perly B and Dalbiez J P 1999 *Carbohydrate Research* **318** 82

[25]   Demé B , Dubois M, Zemb T and Cabane B 1996 *J. Phys. Chem.* **100** 3828

[26]   Demé B and Zemb T 2000 *J. Appl. Crystallogr.* **33** 569

[27]   F. Ricoul , Dubois M and Zemb Th 1997 *J. Phys. II France* 7, 69

[28]   Demé B et al. 1997 *Colloids Surfaces A*, **121** 135

[29]   Cantu L, Corti M, Del Favero E, Dubois M and Zemb T 1998 *J. Phys. Chem. B* **102** 5737

[30]   Bartlett J, Gazeau D, Woolfrey J and Zemb T 1998, *Langmuir* **14** 3538

[31]   Fratini E, Page M G, Giorgi R, Coelfen H, Baglioni P, Demé B and Zemb T, 2007 *Langmuir* **23** 2330.

[32]   Coulombeau H, Testard F, Zemb T and Larpent Ch. 2004 *Langmuir* **12**, 4840

[33]   Erlinger C , Gazeau D, Zemb T, Madic C, Lefrançois L, Hebrant M and Tondre C 1998 *Solvent Ext. Ion Exch.* **16** 707

[34]   Meridiano Y , phD thesis, University of Orsay, Paris XI (France) , 2009

[35]   Nave S, Mandin C, Martinet L, Berthon L, Testard F, Madic C and Zemb T 2003   Physical Chemistry Chemical Physics **6 79**9

[36]   Berthon L, Martinet L, Testard F, Zemb T and Madic C 2007 *Solvent Extraction and Ion Exchange* **25** 545

[37]   Zemb T and Dubois M 2003 *Austr. Australian Journal of Chemistry* **56** 971

[38]   Carrière D, Belloni L, Demé B, Dubois M, Vautrin C and Zemb T 2009 *Small* **5** 1816

[39]   Bäverback P., Oliveira C L P, Garamus v M, Varga I, Claesson P M and Pedersen J S, 2009 *Langmuir* **25**, 7296

[40]   Cecutti C, Focher B, Perly B and Zemb T, 1991 *Langmuir* **7**, 2580

[41]   Ballauff M, 2001 *Curr. Op. in Coll. Interf.* **6**, 132

[42]   Jeng U, Lin T L, Liu W J, Tsao S, Canteenwala T, Chiyang L I, Sung L P, Han C C, 2002 *Physica A*, **304**, 191

[43]   Radlinski A P, mastalerz M, Hinde A L, Hainbuchner M, Rauch M, Baron M, Lin J S, Fan P and Thiyagarajan , 2004, *International journal of coal geology* **59**, 245

[44]   Lesieur P, Lindner P, Desforge C, Lambard J and Zemb T , 1992 *Physica B*, **180**, 564
[45]   Jenkins P J and Donald A M, 1998 *Carbohydrate research* **308**, 133
[46]   Botti A, Pyckhout-Hintzen D, Richter D and Straube E, 2002, *Physica A*, **304**, 230